An evaluation of buckling restrained braced frames with eccentric brace configurations

B. Saxey & C.H. Li
CoreBrace, LLC, West Jordan, Utah, USA

P. Richards
Brigham Young University, Provo, Utah, USA

ABSTRACT

Buckling restrained braced frames (BRBF) are used more frequently than eccentrically braced frames because BRBF are generally more economical while achieving at-least the same level of performance. However, concentric BRBF are less able to accommodate architectural elements such as doors, windows, and corridors. Current US design provisions limit the eccentricities in BRBF to less than the beam depth. The purpose of the present study was to investigate the performance of BRBF with larger brace eccentricities. BRBF were designed with brace eccentricities ranging from 0 (control case) to 2 times the beam depth, and with braces oriented in both chevron and single-diagonal configurations. In each case, the beams were designed to remain elastic under the maximum forces that could be delivered by the braces, including the effects of the brace eccentricity. Nine case-study buildings representing two building heights (12- and 3-story) were considered. Non-linear response history analysis was used to quantify the performance of these design cases under DBE and MCE level shaking. A FEM analysis was performed for verification of member stresses. The key results from the response history analyses were maximum drifts, residual drifts, and brace responses. The paper discusses the relationship between BRBF beam eccentricity and the various response parameters. All the frames responded as designed, with inelasticity confined to the BRBs, and exhibited acceptable behavior. It is recommended that design provisions permit the use of BRBF with beam eccentricities, provided that the beam is designed to prevent yielding and inelasticity is confined to the BRBs.

1 INTRODUCTION

In the late 1970s and through the 1980s, there was a focused research effort to develop a ductile braced frame for U.S. practice. Eccentrically braced frames (EBF) were viewed as a way to combine the stiffness of braced frames with the ductility and architectural flexibility of moment frames. EBF design provisions were included in the original LRFD seismic provisions (AISC 1990) and were updated in subsequent provisions. ASCE 7 recognized the ductility of EBFs with a force reduction factor, R of 8 (ASCE 2016).

Despite their inclusion in seismic provisions for over three decades, EBFs are rarely used in U.S. practice. Buckling-restrained braced frames (BRBF), which also provide high stiffness and ductility (R = 8), have largely replaced EBFs due to their simpler design, lower cost, and fewer detailing requirements. However, BRBFs can lack the architectural flexibility of EBFs. Current AISC seismic provisions (AISC 2022) limit BRBF eccentricities to less than a beam depth, requiring essentially concentric configurations. When project architecture demands greater eccentricity, additional columns can be added to meet code compliance [Fig. 1(a)], but this increases costs and impacts design, underscoring the need for better alternatives.

The seismic provisions (AISC 2022) do not explicitly define "eccentricity" for BRBFs, leading to varying interpretations among engineers. The eccentricity can be measured horizontally ("e_h") or vertically ("e_v"), as illustrated in Figure 1(b). This study defines brace eccentricity using the horizontal measure, e_h. For chevron (Inverted-V) BRBFs [Fig. 1(b)-top], the horizontal eccentricities on either side of the beam mid-span (e_{hL} and e_{hR}) can differ. However, this research focuses on the common case where e_{hL} = e_{hR}.

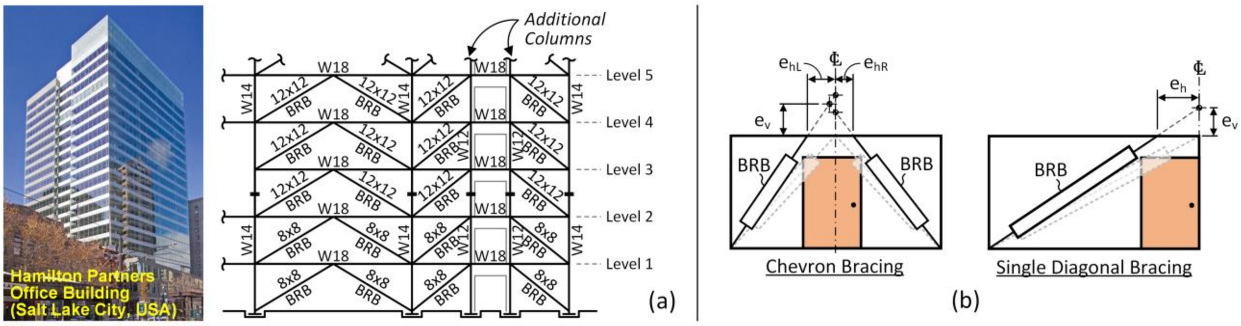

Figure 1: BRBF project where additional columns were added to address the architectural constraints; and (b) various definitions of bracing eccentricity

This study examines BRBFs with eccentricities exceeding current code limits, referred to as BRBF-E. Unlike EBFs using links as the structural fuses, BRBF-E systems are designed with braces as the primary structural fuses, while beams, columns, and other components remain elastic. In chevron BRBF-E [Fig. 2(a)], beams are modelled as pin-ended continuous members. In single-diagonal BRBF-E [Fig. 2(b)], beams consist of two segments: a "stub" rigidly connected to the adjacent column, and a pinned "beam" member between the stub and the opposite column. In this configuration, the stubs and adjacent columns form an elastic "half moment-resisting frame" (half-MRF), which partially resists story shears under lateral forces. With the exception of these "half moment frame" connections, this study focuses on BRBF-E configurations with pin-ended beam connections, representing the "least-stiff" case. In practice, moment connections could replace pin connections to provide additional lateral resistance.

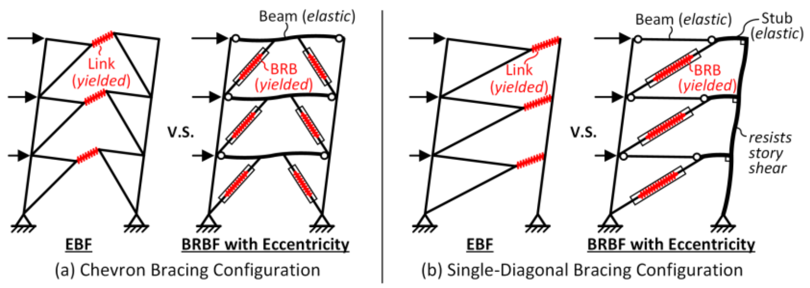

Figure 2: Comparisons in intended plastic mechanism between BRBF-E and EBF for (a) chevron and (b) single-diagonal configurations

This study analytically investigates the seismic design and performance of BRBF-E. Nine case-study buildings are considered in this study. These buildings were analyzed to assess the impact of eccentricities on member sizing and frame weight. Nonlinear analyses, including response history and pushover studies, were conducted to assess seismic performance and design implications.

2 SEISMIC DESIGN OF BRBF WITH ECCENTRICITIES

2.1 Overview and Brace Design

The brace design procedures for BRBF-E are identical to those for concentric BRBF. Braces are sized to remain elastic under the axial demands resulting from the design seismic force effects, determined from the equivalent lateral force (ELF) procedure or modal response spectrum analysis (MRSA) (ASCE 2022). Additionally, the braces are checked to ensure they provide enough stiffness to satisfy drift requirements.

Figure 3(a) illustrates the effect of increasing brace eccentricity on elastic behavior of chevron BRBF-E. Assuming the braces take the entire story shear in the BRBF, the brace axial force (P_{Br}) increases with eccentricity because of the change in brace angle. This results in larger core areas for the braces in BRBF with eccentricity. Despite increasing brace core areas, the BRBF lateral stiffness (K_f) generally decreases with the eccentricity due to the inefficiency of the braces in providing lateral stiffness resulting from the steeper angle and larger beam flexural deflection. The trend of decreasing BRBF lateral stiffness with eccentricity implies that the brace design may be governed by drift when the eccentricity is large.

Figure 3(b) illustrates the effect of increasing brace eccentricity on single-diagonal BRBF-E. The BRBF columns adjacent to the stubs, referred to as Column (C2) members (opposite columns are C1 members), resist a portion of the story shear approximately proportional to the eccentricity-to-span ratio (e/L). As eccentricity increases, the column shear (V_{C2}) rises, reducing the story shear taken by the braces (V_{Br}) and decreasing the brace axial force (P_{Br}). Although the steeper brace angle tends to increase P_{Br}, the reduction in P_{Br} due to the rise in V_{C2} dominates, allowing for smaller brace core areas. Although the reduced core area and steeper angle lower the brace's lateral stiffness, the increased contribution from the half-MRF compensates, slightly boosting the total frame lateral stiffness (K_f). For economical design of single-diagonal BRBF-E, the half-MRF contribution is considered; neglecting it would lead to larger brace core areas and less economical designs due to the steeper brace angle.

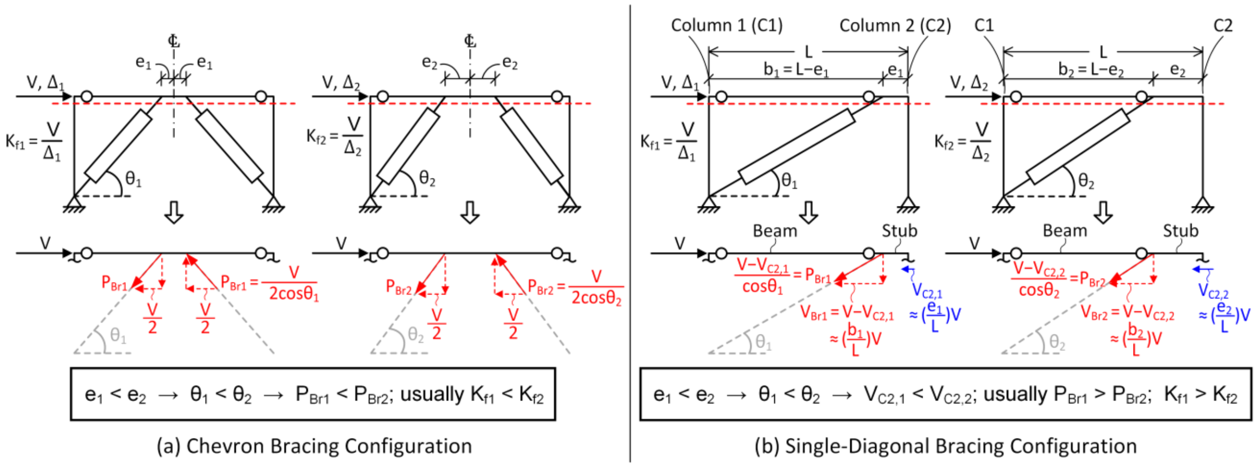

Figure 3: Effects of increasing brace eccentricity on elastic behavior of BRBF-E in (a) chevron and (b) single-diagonal configurations

2.2 Capacity Design

After sizing the braces, BRBF beams and columns are designed using capacity design principles to remain elastic under the force demands induced by the maximum possible brace axial forces, estimated using the code-prescribed adjusted brace strengths (AISC 2022):

$$P_{uT} = \omega F_{ysc} A_{sc};\ P_{uC} = \omega \beta F_{ysc} A_{sc} \tag{1}$$

where P_{uT} and P_{uC} are tension and compression adjusted strengths, respectively. ω is the strain-hardening factor; β is the compression overstrength factor. F_{ysc} is the yield stress, and A_{sc} is the area of the steel core.

For column capacity design, the cumulative effects of simultaneous yielding and development of adjusted strengths for all braces in a BRBF are considered. Beam capacity design accounts for the effects induced by the adjusted brace strengths of the braces. Figure 4 shows that the total force demands [Fig. 4(a)] in the chevron BRBF-E beams come from the superposition of seismic [Fig. 4(b)] and gravity [Fig. 4(c)] effects. In general, the interior beam region (Region 2) experiences high shear and moment and moderate axial force, while the two exterior regions (Regions 1 and 3) are subjected to significant axial and bending.

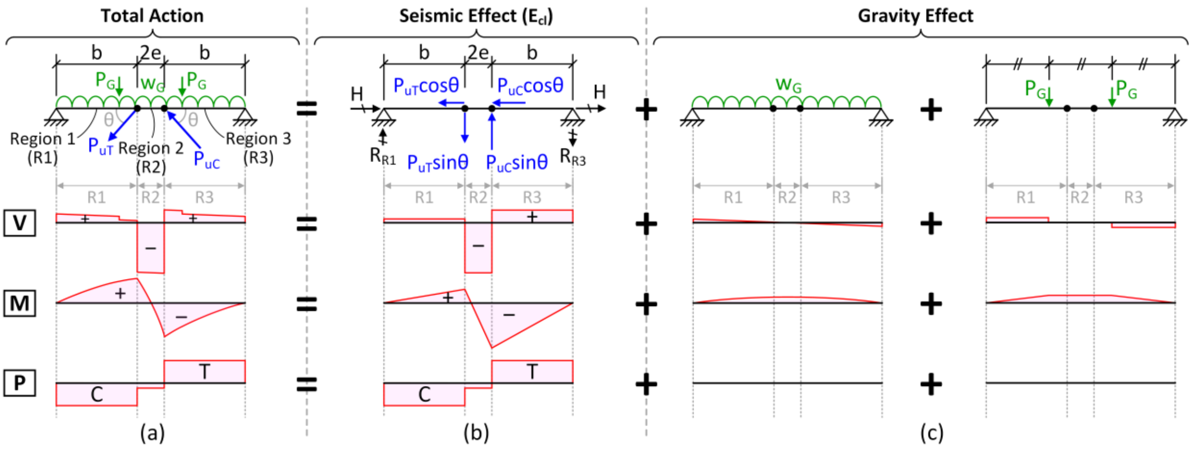

Figure 4: Chevron BRBF-E beam design forces: (a) total from superposition, (b) seismic effects, and (c) gravity effects.

3 CASE STUDY DESIGNS

3.1 Example Building Description

Figure 5 illustrates BRBF designs for nine archetypes adapted from NIST GCR 10-917-8 (NIST 2010). In this study, buildings were designed for seismic design parameters S_{DS} = 1.0 g and S_{D1} = 0.6 g, with an importance factor I_e = 1.0 and a deflection amplification factor C_d = 5, in addition to the gravity loads specified in the NIST report. The archetypes featured two heights (12-story and 3-story), two bracing configurations (chevron and single-diagonal), and various eccentricities. The BRBF design cases are grouped into four categories named 12S-CH, 12S-SD, 3S-CH, and 3S-SD. The prefixes "12S" and "3S" denote the "12-story" and "3-story", respectively, while the suffixes "CH" and "SD" represent the "Chevron" and "Single-diagonal" bracing configurations in the BRBFs. Each group includes two cases: one concentric (C) and one eccentric (E2d), with the eccentricity of twice the nominal beam depth (d_b = 533.4 mm or 21") of W21× beams. Group 12S-CH also has an additional case (E1d) with an eccentricity equal to the beam depth. The "E2d" cases exceed the code limit (AISC 2022), while the "E1d" case adheres to the code's maximum eccentricity allowance. Design cases are named using the group name and eccentricity condition (see Fig. 5).

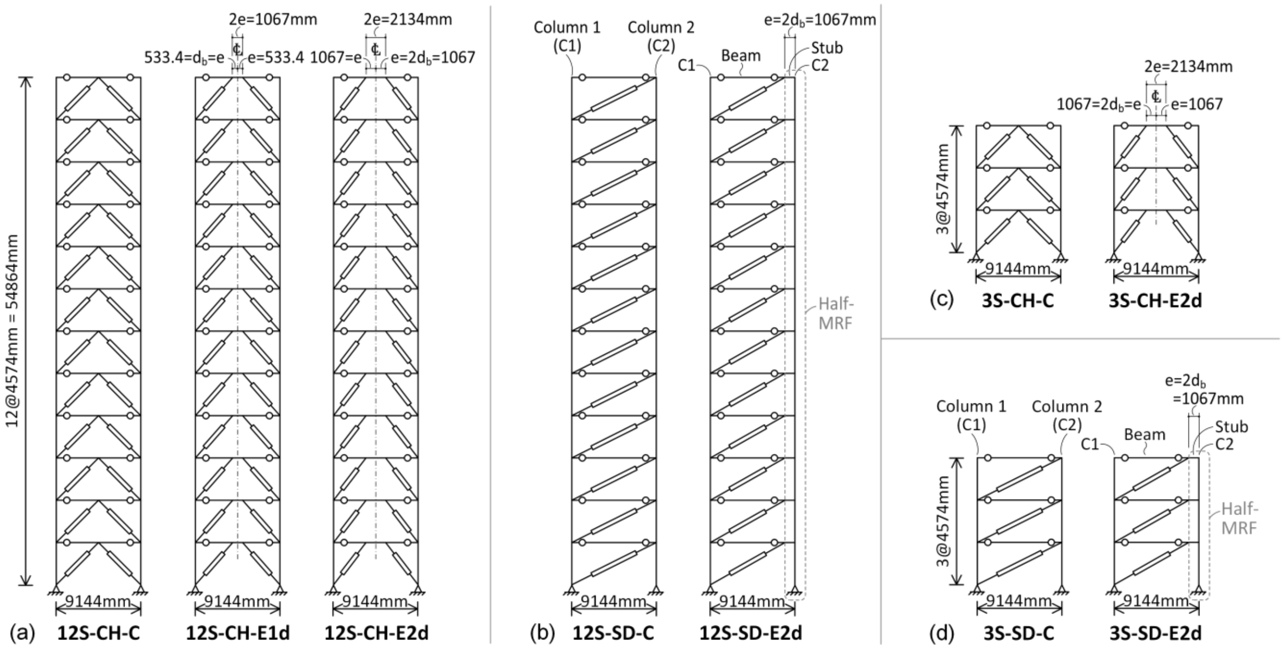

Figure 5: Elevations for BRBF design cases: Groups (a) 12S-CH, (b) 3S-CH, (c) 12S-SD and (d) 3S-SD

Table 1: Member sizes for 3- and 12-story design cases

Member	3-story (3S) BRBF Design Cases				Member	12-story (12S) Design Cases				
	CH-C	CH-E2d	SD-C	SD-E2d		CH-C	CH-E1d	CH-E2d	SD-C	SD-E2d
BRB3 (cm^2)	19	23	29	23	BRB12 (cm^2)	10	10	13	16	13
BRB2 (cm^2)	32	39	52	45	BRB11 (cm^2)	16	16	19	26	23
BRB1 (cm^2)	39	45	65	58	BRB10 (cm^2)	16	19	23	29	26
Bm3	W21×44	W21×68	W21×44	W21×44	BRB9 (cm^2)	19	23	26	32	29
Bm1-Bm2	W21×57	W21×132	W21×83	W21×68	BRB8 (cm^2)	19	23	26	35	32
Stub3	–*	–*	–*	W21×55	BRB7 (cm^2)	23	26	29	39	35
Stub1-Stub2	–*	–*	–*	W21×111	BRB6 (cm^2)	23	26	29	42	39
RC1-RC3†	W14×68	W14×74	W12×79	W14×109	BRB5 (cm^2)	26	29	32	45	42
LC1-LC3†	–‡	–‡	W14×68	W14×61	BRB4 (cm^2)	29	29	32	48	45
					BRB3 (cm^2)	32	32	35	52	48
					BRB2 (cm^2)	35	35	39	55	52
					BRB1 (cm^2)	35	39	42	58	55
					Bm9-Bm12	W21×44	W21×62	W21×83	W21×55	W21×55
					Bm5-Bm8	W21×44	W21×68	W21×101	W21×68	W21×62
					Bm1-Bm4	W21×50	W21×83	W21×122	W21×73	W21×68
					Stub9-Stub12	–*	–*	–*	–*	W21×68
					Stub5-Stub8	–*	–*	–*	–*	W21×93
					Stub1-Stub4	–*	–*	–*	–*	W21×111
					RC11-RC12†	W14×43	W14×38	W14×34	W14×43	W14×48
					RC9-RC10†	W14×68	W14×68	W14×68	W14×82	W14×82
					RC7-RC8†	W14×109	W14×109	W14×109	W14×109	W14×120
					RC5-RC6†	W14×132	W14×132	W14×145	W14×145	W14×159
					RC3-RC4†	W14×176	W14×176	W14×193	W14×193	W14×211
					RC1-RC2†	W14×233	W14×233	W14×233	W14×257	W14×257
					LC1-LC12†	–‡	–‡	–‡	–§	W14×38
					LC9-LC10†	–‡	–‡	–‡	–§	W14×68
					LC7-LC8†	–‡	–‡	–‡	–§	W14×109
					LC5-LC6†	–‡	–‡	–‡	–§	W14×145
					LC3-LC4†	–‡	–‡	–‡	–§	W14×193
					LC1-LC2†	–‡	–‡	–‡	–§	W14×257

*Stubs are not used
†In single-diagonal BRBFs, the left column (LC) and right column (RC) are Column 1 (C1) and Column 2 (C2), respectively.
‡The same shape is used for RC and LC as the force demands in both sides of columns are identical in chevron BRBFs.
§The demands in LC and RC are different, but the same shape is used for both sides as the demand difference is not large.

3.2 Steel Weight Comparison

Table 1 summarizes overall frame design results, while Tables 2 present the steel weights for the 12- and 3-story case study designs, respectively. For chevron BRBF cases, the brace steel weights (including casing but excluding infill grout) were similar across the12-story cases (12S-CH-C, 12S-CH-E1d, and 12S-CH-E2d) and the 3-story cases (3S-CH-C and 3S-CH-E2d). This similarity reflects how shorter brace lengths and casing weights offset core area increases due to eccentricity. Column weights within each chevron group were also similar, as column sizes only slightly increased with eccentricity. However, beam weights were significantly heavier in eccentric cases, resulting in a total steel weight increase with eccentricity in chevron BRBFs. For 12-story group, Cases 12S-CH-E1d and 12S-CH-E2d were 1.10 and 1.27 times heavier, respectively, than 12S-CH-C. Similarly, 3-story group, 3S-CH-E2d was 1.32 times heavier than 3S-CH-C.

In single-diagonal BRBF design cases, eccentric frames required significantly less brace steel weight than concentric frames. For example, Case 12S-SD-E2d was 18% lighter than 12S-SD-C, and 3S-SD-E2d was 24% lighter than 3S-SD-C. This reduction is due to C2 columns in eccentric BRBFs resisting part of the story shear, reducing brace axial demands. Shorter brace lengths from steeper angles further reduced brace steel weight. Column weights were slightly higher in eccentric cases, as increases in C2 column weight were partially offset by reductions in C1 column weight. Beam weights were slightly lower in eccentric frames because lighter sections were used for long-span beam members despite heavier stub sections. Overall, 12S-SD-E2d was 3% lighter than 12S-SD-C, while 3S-SD-E2d was 5% lighter than 3S-SD-C.

Alternative designs for single diagonal BRBF-E neglecting the half-MRF contribution (denoted as 12S-SD-E2d* and 3S-SD-E2d* in Tables 2) required larger braces, heavier beams, and columns. These "re-designs" resulted in a total weight 6% higher for 12S-SD-E2d* compared to 12S-SD-C and 4% higher for 3S-SD-E2d* compared to 3S-SD-C. This demonstrates that ignoring half-MRF action in single-diagonal BRBF-E designs leads to increased steel weight.

Table 2: Steel weights for design cases

Group	Design	BRB (tonf)	Column (tonf)	Beam (tonf)	Frame (tonf)	Frame + BRB (tonf)	Increase (%)
12S-CH	12S-CH-C	7.46	20.38	7.39	27.78	35.23	−
	12S-CH-E1d	7.25	20.25	11.41	31.66	38.91	+10.44%
	12S-CH-E2d	7.33	20.95	16.39	37.34	44.67	+26.79%
12S-SD	12S-SD-C	9.48	22.21	10.50	32.71	42.19	−
	12S-SD-E2d	7.76	22.59	10.45	33.05	40.81	−3.27%
	12S-SD-E2d*	8.62	25.00	11.09	36.10	44.72	+5.99%
3S-CH	3S-CH-C	2.16	2.73	2.12	4.85	7.01	−
	3S-CH-E2d	2.12	2.97	4.18	7.15	9.27	+32.28%
3S-SD	3S-SD-C	2.78	2.95	2.81	5.77	8.54	−
	3S-SD-E2d	2.12	3.42	2.56	5.98	8.09	−5.24%
	3S-SD-E2d*	2.37	3.78	2.73	6.50	8.88	+3.91%

Table notes: The BRB weight includes steel core, lug plates, and casing, excluding infill concrete. For beam and column weight calculations, centerline lengths were multiplied by the shape weight/length. Stiffeners and gussets plate weights were not considered.

4 RESPONSE HISTORY ANALYSIS STUDY

4.1 Modelling

Non-linear response history analysis (NLRHA) was conducted to evaluate the seismic performance of case-study buildings. 16 ground motion records selected from FEMA P-695 far-field set (ATC 2009) were scaled to Design Basis Earthquake (DBE) and Maximum Considered Earthquake (MCE) levels and used as the input motions. This study focuses on the mean structural responses, such as peak story drifts and brace core strains, averaged across the 16 records, with MCE results presented in this paper.

As shown in Figure 6(a), OpenSees (Mazzoni et al., 2006) was used to model the BRBF design cases. Each BRBF model was tied to a fishbone system (Lignos et al., 2013) representing the gravity framing, incorporating the lateral stiffness of the gravity beam-to-column connections. Gravity loads and seismic masses were applied to the fishbone system. For the BRBF portion, beam-to-column intersections were modelled as rigid joints and pins were introduced in the beam to represent bolted connections. Offset elements modelled stiffened panel zones and corner gussets, assigned flexural properties ten times those of the framing members. Base connections were pinned.

BRBF beams and columns were modelled as elastic beam-column elements, and their forces were checked using NLRHA to ensure they remained within elastic limits. Resistance from gravity connections was modelled using nonlinear hinges with Pinching4 material (Lowes et al., 2003) to represent the lumped properties of shear tab connections with parameters calibrated per ATC-114/NIST guidelines (NIST 2017). Second-order effects were included both locally in the braced frame and globally through the leaning column in the fishbone model. 2% Rayleigh damping was set at the first and third mode periods.

Buckling restrained braces (BRB) were modelled as corotational truss, with an expected core yield strength, $F_{ysc,e}$, of 290 MPa (42 ksi). The hysteretic behavior was defined using the Menegatto-Pinto steel material (SteelMPF) incorporating isotropic strain hardening. Initial stiffness was defined by the effective stiffness factor, KF. Cyclic properties were calibrated to match the adjusted strengths, P_{uT} and P_{uC}, at the expected deformation (either the brace deformation at a 2% story drift or twice the required design displacement) per AISC 341 (AISC 2022). Figure 6(b) illustrates a calibrated BRB material and backbone targets.

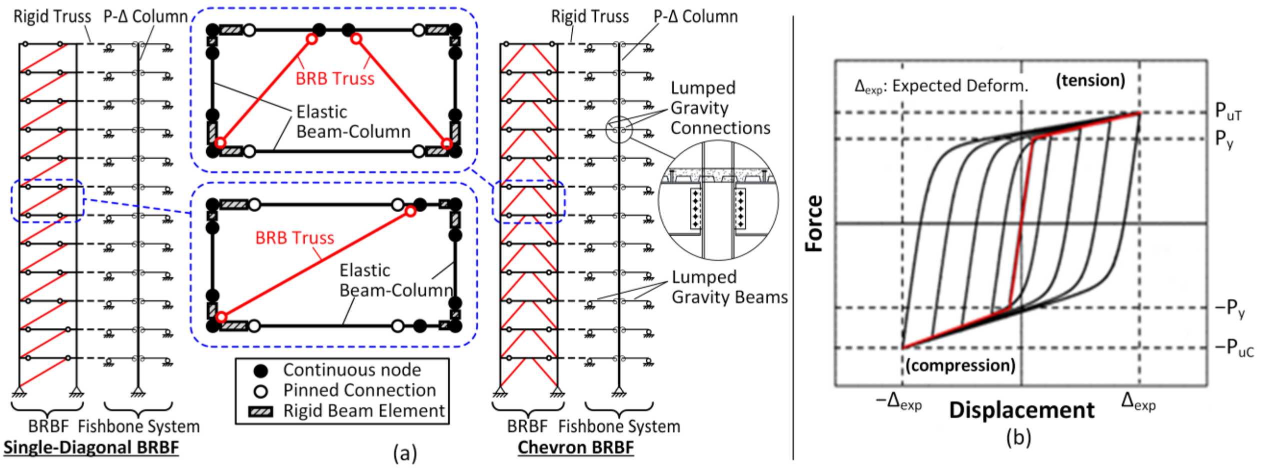

Figure 6: OpenSees modelling methods: (a) elements and constraints, (b) BRB modelling and calibration.

4.2 Analysis Results

4.2.1 Story Drift Response

Figure 7(a) shows the mean peak story drifts from NLRHA at MCE level. All design cases exhibit peak story drifts below the MCE drift limits prescribed in ASCE 7 (ASCE 2022). Similarly, the DBE story drift ratios for all cases remain within the ASCE 7 limit of 0.02, confirming the code-compliant seismic performance of these designs. For chevron BRBFs [Figs. 7(a1) and 7(a2) for Groups 12S-CH and 3S-CH, respectively], the peak story drift for the eccentric case generally surpasses those of the concentric case at the lower stories, where the largest drifts occurred. However, as seen in Fig. 7(a1), some intermediate-story drifts in the 12-story eccentric cases (12S-CH-E1d and 12S-CH-E2d) are less than those in the concentric case (12S-CH-C).

On the other hand, for single-diagonal BRBFs, the peak story drift response generally decreases with increasing brace eccentricity. For 12-story design cases [Fig. 7(a3)], the MCE story drift response in the eccentric Case 12S-SD-E2d is noticeably less than that in the concentric case 12S-SD-C for the lower half of the frame. Similarly, for the 3-story design cases [Fig. 7(a4)], the MCE story drifts in 3S-SD-E2d are also smaller than those in 3S-SD-C, albeit to a lesser extent. This reduction in drifts for the single-diagonal BRBF-E can be attributed to the half-MRF [Figs. 3(b) and 3(d)], which acts as an elastic backup lateral system providing stiffness after the braces yield and reducing the inelastic story drifts of the frame.

It is noted that, Figures 7(a3) and 7(a4) also display the responses of additional design cases, 12S-SD-E2d* and 3S-SD-E2d*, which represent alternative designs for Cases 12S-SD-E2d and 3S-SD-E2d, respectively. In contrast to the proposed design for 12S-SD-E2d and 3S-SD-E2d, where the contribution from C2 members in resisting story shear is considered, the alternative designs for 12S-SD-E2d* and 3S-SD-E2d* follow the conventional practice of assuming the entire story shears are carried by the braces only. This conventional approach leads to more conservative design results, with all member sizes for the braces, beams, and columns in the alternative design cases being larger than those in their counterpart benchmark design cases. As shown in Figures 7(a3) and 7(a4), the alternative design Cases 12S-SD-E2d* and 3S-SD-E2d* generally exhibit smaller story drift responses compared to 12S-SD-E2d and 3S-SD-E2d.

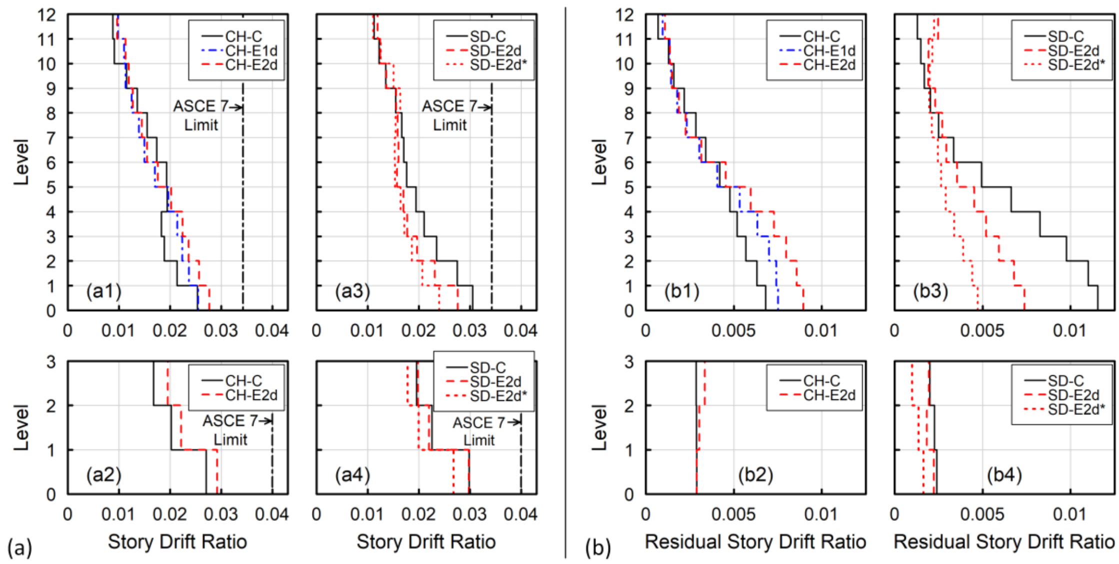

Figure 7: MCE-level BRBF responses: (a) peak story drifts and (b) residual story drifts

Figure 7(b) shows the residual story drift responses following MCE-level loading. For Group 12S-CH [Fig. 7(b1)], the residual story drifts in the lower stories of the eccentric cases (12S-CH-E1d and 12S-CH-E2d) are noticeably higher than those in the concentric case (12S-CH-C), with the response in 12S-CH-E2d generally exceeding that of 12S-CH-E1d. For Group 3S-CH [Fig. 7(b2)], the residual story drifts in 3S-CH-E2d are slightly higher than those in 3S-CH-C, despite similar first-story response in both cases. These analysis results indicate that, for chevron BRBFs, residual story drifts tend to increase with brace eccentricity

In contrast, the single-diagonal BRBF-E cases show noticeably smaller residual drifts compared to their concentric counterparts. For Group 12S-SD [Fig. 7(b3)], the residual story drifts in 12S-SD-E2d are considerably lower than those in 12S-SD-C, particularly in the lower stories. Similarly, for Group 3S-SD [Fig. 7(b4)], residual story drifts along the entire height of 3S-SD-E2d are smaller than those in 3S-SD-C. Furthermore, as shown in both Figures 7(b3) and 7(b4), the alternative design cases 12S-SD-E2d* and 3S-SD-E2d*, with heavier frame members, exhibit even further reductions in residual story drift response.

In summary, the analysis results suggest that eccentric configurations for single-diagonal BRBFs are an efficient way to reduce story drifts, particularly residual drifts. Notably, the eccentric cases (12S-SD-E2d and 3S-SD-E2d) are lighter than their concentric counterparts by about 3% and 5%, respectively, while providing improved control over story drift responses. When applying the conventional, but conservative, design approach, the additional eccentric cases (12S-SD-E2d* and 3S-SD-E2d*) exhibit further enhanced seismic performance in controlling story drifts, with only a modest weight increase of about 6% and 4%, respectively).

4.2.2 Brace Response

Plots of peak BRB core strains from the NLRHA at MCE level are shown in Figure 8(a). Overall, the peak BRB strains are below the expected values corresponding to a story drift ratio of 0.02 at all levels, except at the bottom three stories in the 12-story cases [Figs. 8(a1) and 8(a3)] and the ground floor in the 3-story cases [Figs. 8(a2) and 8(a4)], where higher strains (up to 2.44%) are observed. These strain demands, however, remain within experimental BRB deformation capacities, which typically exceed 3% strain. When comparing eccentric and concentric frames, a trend indicates that eccentric frames generally develop moderately higher BRB core strains than their concentric counterparts, especially in braces experiencing the highest strains. For Groups 12S-SD, 3S-CH, and 3S-SD, nearly all BRB strains in the eccentric frames exceed those in their concentric frames. For Group 12S-CH [Fig. 8(a1)], the two eccentric cases (12S-CH-E1d and 12S-CH-E2d) exhibit higher BRB core strains at the bottom four stories than the concentric case (12S-CH-C), while smaller strains were observed in the upper stories.

The BRB normalized ultimate force represents the ratio of the maximum compressive force, P_u, in a BRB from the NLRHA to its expected yield force, P_{ye}, calculated as the product of the yielding core area (A_{sc}) and the expected yield stress ($F_{ysc,e}$). This parameter quantifies the overstrength, $\omega\beta$, seen in the BRB. The plots of the peak BRB normalized forces at MCE levels are presented in Figure 8(b). The brace overstrength correlates closely with the core strain response, leading to similar trends between BRB core strains and normalized ultimate forces. The results show that the BRB normalized ultimate forces are below the expected overstrength $\omega\beta$ values used for design, except at the bottom three stories in the 12-story cases [Figs. 8(b1) and 8(b3)] and the ground floor in the 3-story cases [Figs. 8(b2) and 8(b4)]. At these levels, the observed overstrength exceeded the expected values by approximately 9.7% in the 12-story cases and 12.4% in the 3-story cases, primarily in the first story where the highest overstrength occurred.

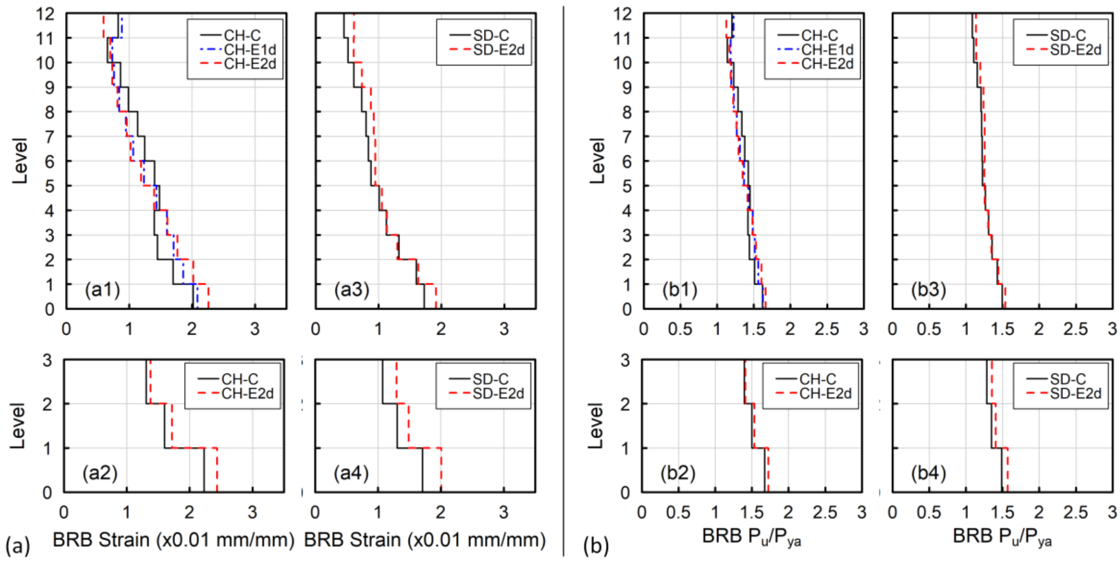

Figure 8: MCE-level BRB responses: (a) peak core strains and (b) peak normalized axial forces

5 FINITE ELEMENT ANALYSIS STUDY

Finite element simulations were performed using ANSYS (ANSYS 2022) to investigate the stress state in BRBF-E beams when braces reach design deformations. Displacement-controlled pushover analyses ramped to a 2% story drift were performed on individual frame models that explicitly considered the beam and gusset geometry in the connection region. Two single-story frames—BRBF-CH-E1d and BRBF-CH-E2d—were analyzed, based on the first-story designs of the 12-story chevron case study frames (12S-CH-E1d and 12S-CH-E2d; see Table 1 for member sizes). As shown in Figure 9(a), the models employed three element types: solid hexahedral elements (SOLID186) for the gusset and beam in the connection region, elastic beam elements (BEAM188) for the beam outside the gusset region and the columns, and non-linear springs (COMBIN39) for the BRBs. Boundary conditions included pinned column base nodes, fully restrained beam-to-column connections (to reflect gusset plates from the story above, not modeled), and pinned brace connections. The frames were constrained against out-of-plane displacements.

Figures 9(b) and 9(c) show the displaced geometry and the Equivalent (von Mises) stress in the connection region, for the two BRBF-E models (BRBF-CH-E1d and BRBF-CH-E2d) at 2% story drift. In Figure 9(b), BRBF-CH-E1d (W21×83 beam) exhibits a peak Equivalent stress reached 243.6 MPa (35.3 ksi) in the central region of the beam web, primarily caused by beam shears from the eccentricity, which were accounted for in the design. The design procedure, as schematized in Figure 4, conservatively neglected any shear contribution from the gusset plate. This approach effectively prevents the beam from reaching a yielding limit state. In Figure 9(b) BRBF-CH-E2d, (W21×122 beam) demonstrates a peak Equivalent stress well below 345 MPa (50 ksi), reaching only 204.2 MPa (29.6 ksi) in the central region of the beam web, further validating the reasonableness of the adopted design approach.

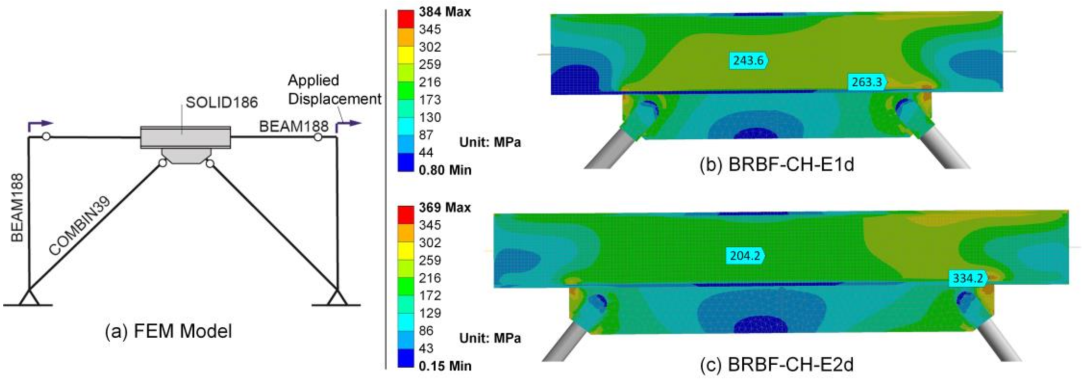

Figure 8: (a) FEM model and Equivalent (von Mises) stress contours in the connection regions at 2% story drift for Models (b) BRBF-CH-E1d and (c) BRBF-CH-E2d

6 CONCLUSIONS

Based on the analysis results in this study, the following conclusions can be drawn:

- The NLRHA results demonstrate that the BRBFs with eccentricities that perform well during the DBE and MCE-level earthquakes with story drifts lower than the code-prescribed prescribed limit. The results confirm the satisfactory seismic performance of BRBFs having eccentricities equal to twice the beam depth, (exceeding the current code limit of one beam depth), provided they are properly capacity-designed such that the beams and columns remain elastic, confining inelasticity to the BRBs.
- Chevron BRBFs show a slight increase in peak and residual drifts with increasing eccentricity, particularly in the lower stories. In contrast, single-diagonal BRBFs with eccentric configurations experience significantly lower peak and residual drifts compared to concentric frames, with a

pronounced reduction in residual drifts. This improvement stems from the half-MRF formed by the stubs and adjacent columns, which provides an elastic backup lateral system for single-diagonal BRBF-E.

- Detailed finite element pushover analyses confirm that the proposed capacity design method for chevron BRBF beams with eccentricity effectively prevents local stress concentration issues near the brace-to-beam intersection, even without explicitly accounting for local stress distributions.

7 REFERENCES

ASIC (2016). "*Seismic Provisions for Structural Steel Buildings*". ANSI/AISC 341-16, American Institute of Steel Construction, Chicago, IL, USA.

ASIC (2022). "*Seismic Provisions for Structural Steel Buildings*". ANSI/AISC 341-22, American Institute of Steel Construction, Chicago, IL, USA.

ANSYS (2022). "*Ansys Mechanical, Release 22.1, Help System*". ANSYS, Inc., Canonsburg, PA, USA.

ASCE (2016). "*Minimum Design Loads and Associated Criteria for Buildings and Other Structures*". ASCE/SEI 7-16, American Society of Civil Engineers, Reston, VA, USA.

ASCE (2022). "*Minimum Design Loads and Associated Criteria for Buildings and Other Structures*". ASCE/SEI 7-22, American Society of Civil Engineers, Reston, VA, USA.

ATC (2009). "*Quantification of Building Seismic Performance Factors*". FEMA P-695, Federal Emergency Management Agency, Washington D.C., USA.

Lignos, DG, Putman, C, Krawinkler, H (2013). "Seismic Assessment of Steel Moment Frames using Simplified Nonlinear Models, Computational Methods in Earthquake Engineering". *Computational Methods in Applied Sciences book series*, **30**: 91-109.

Lowes, LN, Mitra, N and Altoonash, A (2003). "*A Beam-Column Joint Model for Simulating the Earthquake Response of Reinforced Concrete Frames*". Report No. 2003/10 Pacific Earthquake Engineering Research Center, Berkeley, CA, USA.

Mazzoni, S, McKenna, F, Scott, M and Fenves, G (2006). "*OpenSees Command Language Manual*". Pacific Earthquake Engineering Research Center, Berkeley, CA, USA.

NIST (2010). "*Evaluation of the FEMA P-695 Methodology for Quantification of Building Seismic Performance Factors*". NIST GCR 10-917-8, National Institute of Standards and Technology, Gaithersburgh, MD, USA.

NIST (2017). "*Recommended Modeling Parameters and Acceptance Criteria for Nonlinear Analysis in Support of Seismic Evaluation*". NIST GCR 17-917-45, National Institute of Standards and Technology, Gaithersburgh, MD, USA.